Carbohydrate Polymers 117 (2015) 468–475

Contents lists available at ScienceDirect

Carbohydrate Polymers

journal homepage: www.elsevier.com/locate/carbpol

Preparation, characterization, and antimicrobial activity of chitin nanofibrils reinforced carrageenan nanocomposite films

Shiv Shankar[a], Jeevan Prasad Reddy[a], Jong-Whan Rhim[a,*], Hee-Yun Kim[b]

[a] Department of Food Engineering and Bionanocomposite Research Institute, Mokpo National University, 61 Dorimri, Chungkyemyon, Muangun, Jeonnam 534-729, Republic of Korea
[b] Department of Food Service Management, Woosong University, 171 Dongdaejeon-ro, Dong-gu, Daejeon 300-715, Republic of Korea

ARTICLE INFO

Article history:
Received 27 July 2014
Received in revised form 7 October 2014
Accepted 7 October 2014
Available online 17 October 2014

Keywords:
Chitin
Nanofibrils
Carrageenan
Nanocomposite films
Antimicrobial activity

ABSTRACT

Present study illustrates the preparation of chitin nanofibrils (CNF) reinforced carrageenan nanocomposite films by the solution-casting technique. CNF was prepared by acid hydrolysis of chitin, followed by high speed homogenization and sonication. FTIR result demonstrated that the chemical structure of chitin had not changed after acid hydrolysis. However, the crystalinity of CNF was found to be higher than chitin. The crystallite size of chitin and CNF was 4.73 and 6.27 nm, respectively. The char content at 600 °C of chitin (19.2%) was lower than the CNF (25%). The carrageenan/CNF composite films were smooth and flexible and the CNF was dispersed uniformly in the carrageenan polymer matrix. The tensile strength and modulus of carrageenan film were increased significantly ($p < 0.05$) after CNF reinforcement with up to 5 wt%, however, elongation at break, water vapor permeability, and transparency decreased slightly. Carrageenan/CNF nanocomposite films showed strong antibacterial activity against a Gram-positive food-borne pathogen, *Listeria monocytogenes*.

1. Introduction

Concerns on the environment and exhaust of natural resources caused by the non-biodegradable petroleum-based plastics have attracted attention on the development of environmentally benign polymers and polymer nanocomposites for the applications in food packaging and other value added utilities. Renewable and abundantly available biopolymers are the most viable alternative for the production of green materials in the near future. Nature has provided various natural biopolymers such as polysaccharides (cellulose, starch, and chitosan) and proteins (soy protein, wheat protein, casein, and gelatin). Utilization of natural biopolymers for making biodegradable packaging films, edible film, and coating materials have been increased considerably in the past decades (Rhim, Park, & Ha, 2013). Among such natural biopolymers, carrageenan is one of the promising biopolymers since it is abundantly obtained from renewable resources such as red edible seaweeds, which has strong gel forming ability, biocompatibility, and is environmentally friendly. Carrageenan is a linear sulfated polysaccharide extracted from various species of the *Rhodophyta* (marine red algae) (Necas & Bartosikova, 2013). Carrageenan has been frequently used to prepare biodegradable or edible packaging films. However, poor performances such as lower water vapor barrier and relatively lower mechanical properties are the main limitations of such biopolymer-based films. To overcome these problems, a number of research works have been performed by reinforcing nanofiller materials (Martins et al., 2013; Rhim, Park, & Ha, 2013). Inorganic (metallic nanoparticles, and nanoclays) or organic (cellulose nanowhiskers, starch nanoparticles, and chitosan nanoparticles) nanofillers have been used as reinforcing materials. Reinforcement of organic nanofillers is preferred over inorganic nanofillers because of their completely biodegradable nature.

Among all organic nanofillers, chitin nanofibrils (CNF) is one of the most promising nanofiller. Chitin is a linear polysaccharide, made up of β-(1-4)-linked 2-acetamido-2-deoxy-D-glucopyranose units which may be deacetylated to some extent (Muzzarelli, 2011a). Chitin is the second most abundant biomaterial after cellulose in the world. Chitin can be obtained from the cell wall of fungi, the exoskeleton of arthropods such as crustaceans (e.g., crabs, lobsters, and shrimps) and insects, the radula of molluscs, and the beaks and the internal shells of cephalopods including squids and octopuses (Muzzarelli, 2011a, Muzzarelli et al., 2012)Chitin upon acid hydrolysis can form crystalline nanofibrils and nanowhiskers, which have been recently explored in nanotechnology applications (Mincea, Negrulescu, & Ostafe, 2012; Muzzarelli, 2011b). Marine chitin lends itself to the isolation of nanofibrils, otherwise

* Corresponding author. Tel.: +82 61 450 2423; fax: +82 61 454 1521.
E-mail addresses: jwrhim@mokpo.ac.kr, jwrhim@hanmail.net (J.-W. Rhim).

http://dx.doi.org/10.1016/j.carbpol.2014.10.010
0144-8617/

called nanocrystals or whiskers; this matter has been the subject of various review articles (Mincea et al., 2012; Muzzarelli, 2011a; Muzzarelli, 2011b; Muzzarelli, 2012; Muzzarelli et al., 2012). Reports are available on the formations of chitin whiskers using acid hydrolysis (Ifuku et al., 2009; Revol & Marchessault, 1993), however, few studies have been reported on the preparation of biopolymer-based films reinforced with chitin nanofibrils. To the best of our knowledge, reports on the reinforcement of carrageenan-based biopolymer films with chitin nanofibrils (CNF) have not been available in the literature.

The main objective of the present study was to synthesize CNF from chitin and preparation of carrageenan/CNF nanocomposite films. The CNF was characterized by various analytical techniques. The effects of CNF concentrations on the optical, mechanical, and water vapor barrier properties of carrageenan/CNF nanocomposite films were studied.

2. Materials and methods

2.1. Materials

Food grade carrageenan (HGE-A, pure κ-carrageenan, viscosity [1.5% aq. solution at 75 °C] 60 cps) was obtained from MSC Co. Ltd. (Sungnam city, Kyunggido, Korea). Glycerol and hydrochloric acid (HCl) were purchased from Sigma-Aldrich (St Louis, MO, USA). Chitin (viscosity [0.5%-AA & CS at 20 °C]: 800–940 cps, ash < 5%, particle size: 3 mm) obtained from crab shell was procured from YB Bio Co., Ltd. (Youngduk, Kyungbuk, Korea) and used without any modification. Food-borne pathogenic bacteria, *Escherichia coli* O157:H7 ATCC 43895 and *Listeria monocytogenes* ATCC 15313, were obtained from Korean Collection for Type Cultures (KCTC, Seoul, Korea). The bacterial strains were cultured in tryptic soy broth (TSA) and brain heart infusion broth (BHI) agar media and subsequently stored at 4 °C for further analysis.

2.2. Isolation of chitin nanofibrils

Chitin nanofibrils (CNF) were isolated from the chitin by acid hydrolysis. For this, 5 g of chitin was hydrolyzed with 3 N HCl (chitin to acid ratio of 1:20) by refluxing for 3 h at 60 °C under strong agitation. The reaction was quenched by adding an excess of distilled water to the reaction mixture and the resulting mixture was cooled to the room temperature. The unhydrolyzed fibers were filtered and the filtrate was centrifuged at 4000 rpm for 20 min using a bench-top centrifuge (Hanil Scientific Centrifuge, Incheon, Kyonggido, Korea). The precipitate obtained was repeatedly washed with distilled water and the supernatant was discarded until it became turbid. During this process, the pH of the suspension was above 5. Thereafter, the suspension was homogenized using a high speed homogenizer (T25 basic, Ika Labotechnik, Janke & Kunkel Gmbh & Co., KG Staufen, Germany) at 7000 rpm for 30 min followed by sonication for 5 min in an ice bath using a high intensity ultrasonic processor (Model VCX 750, Sonics & Materials Inc., Newtown, CT, USA). Finally, the suspension was subjected to dialysis against distilled water until neutral pH was attained. The suspension was stored in a refrigerator at 4 °C for further analysis.

2.3. Preparation of films

Carrageenan and carrageenan/CNF nanocomposite films with different concentration of CNF (3, 5, and 10 wt% based on carrageenan) were prepared using a solution casting method (Rhim, 2011). For this, predetermined amount of CNF was dispersed in 150 mL of distilled water and stirred for 1 h using a magnetic stirrer. The fully wetted suspensions were homogenized using a high shear mixer (T25 basic, Ika Labotechnik, Janke & Kunkel Gmbh & Co., KG Staufen, Germany). Thereafter, 1.2 g of glycerol was mixed in the suspension as a plasticizer and mixed vigorously for 20 min on a magnetic stirrer. Then, 3 g of carrageenan was added slowly in the above solution and mixed vigorously for 30 min at 95 °C using a magnetic stirrer and cast evenly onto a leveled Teflon film (Cole-Parmer Instrument Co., Chicago, IL, USA) coated glass plate ($24 \times 30\ cm^2$). The films were allowed to dry for about 24 h at room temperature. The dried films were peeled off from the casting plates and conditioned in a constant temperature humidity chamber set at 25 °C and 50% relative humidity (RH) for at least 48 h before further analysis. The control film of carrageenan (without CNF) was also prepared following the same method described above.

2.4. Characterization

Particle size of CNF was analyzed using a particle size analyzer (Brookenhaven Instruments Corp., New York, USA). 20 μL of homogeneous CNF suspension was diluted into 3 mL of deionized distilled water and subjected to the particle size analyzer.

Fourier transform infrared (FT-IR) spectra of chitin and CNF were obtained using an attenuated total reflectance-Fourier transform infrared (ATR-FTIR) spectrophotometer (TENSOR 37 Spectrophotometer with OPUS 6.0 software, Billerica, MA, USA) in the range of $4000–500\ cm^{-1}$.

X-ray diffraction (XRD) pattern of chitin, CNF and carrageenan/CNF nanocomposite films was analyzed using a PANalytical Xpert pro MRD diffractometer (Amsterdam, Netherlands). The XRD spectra were recorded using Cu-Kα radiation (wavelength of 0.1546 nm) and a nickel monochromator filtering wave at a voltage and current of 40 kV and 30 mA, respectively. The diffraction patterns were obtained at diffraction angles between 5 and 50° with a scanning rate of 0.4°/min at room temperature. The degree of crystallinity (DC) of chitin and CNF was calculated using following equation (El-Nesr, Raafat, Nasef, Soliman, & Hegazy, 2013):

$$DC = (I_{110} - I_{am})/I_{110} \quad (1)$$

where, I_{110} is the intensity of the peak at (110) lattice (at $2\theta = 19.1°$) and I_{am} is the intensity of the peak at $2\theta = 16°$ (amorphous region). And the crystallite size (D) of the fiber was calculated by using the Scherrer equation (Das et al., 2009).

$$D = K\lambda/\beta_{1/2}\cos\theta \quad (2)$$

where, K is a constant (0.94), λ is the *X*-ray wavelength ($\lambda = 0.154056$ nm), $\beta_{1/2}$ is the full width at the half maximum of the deflection peak (FWHM), and θ is Bragg's angle.

The microstructure of chitin and CNF and the surface morphology of carrageenan/CNF nanocomposite films were observed using a field emission scanning electron microscopy (FE-SEM, S-4800, Hitachi Co., Ltd., Matsuda, Japan) operated with an acceleration voltage of 10 kV and current of 10 μA after coating the samples with platinum (Pt) using a vacuum sputter coater.

2.5. Thermal stability

Thermal stability of chitin and CNF was determined by thermogravimetric analyzer (Hi-Res TGA 2950, TA Instrument, New Castle, DE, USA). For this, about 5 mg of sample was taken in a standard aluminum cup and heated from 30 to 600 °C at heating rate of 10 °C/min under a nitrogen flow of $50\ cm^3$/min. An empty cup was used as a reference.

2.6. Color and transparency

The surface color of the films was measured using a Chroma meter (Konica Minolta, CR-400, Tokyo, Japan). A white standard

color plate ($L = 97.75$, $a = -0.49$ and $b = 1.96$) was used as a background for color measurements. Hunter color (L, a, and b) values were averaged from five readings from each sample. The total color difference (ΔE) was calculated as follows:

$$\Delta E = \sqrt{(\Delta L)^2 + (\Delta a)^2 + (\Delta b)^2} \quad (3)$$

where, ΔL, Δa, and Δb are differences between each color value of standard color plate and film specimen, respectively.

The percent transmittance at wavelength of 660 nm (T_{660}) was determined using a UV/vis spectrophotometer (Model 8451A, Hewlett-Packard Co., Santa Alara, CA, USA) (Rhim, 2012).

2.7. Tensile properties

Thickness of films was determined using a micrometer (Dial thickness gauge 7301, Mitutoyo, Japan) at an accuracy of 0.01 mm. Five random measurements were taken for each film and the average values were used as the film thickness. Tensile properties such as tensile strength (TS), elongation at break (E), and elastic modulus (EM) of each film were measured according to the standard test method of ASTM D 882-88 using Instron Universal Testing Machine (Model 5565, Instron Engineering Corporation, Canton, MA, USA). Film sample was cut into rectangular strips (2.54 cm × 15 cm) using a precision double blade cutter (Model LB.02/A, Metrotech, SA, San Sebastain, Spain). The testing machine was operated in tensile mode with an initial grip separation of 50 mm and crosshead speed of 50 mm/min. The TS (Pa) was determined by dividing the maximum load (N) by the initial cross-sectional area (m^2) of the film. The E (%) was determined by dividing the extension at the rupture of the film by the initial length of the film (50 mm) multiplied by 100, and the EM (GPa) was determined from the slope of the linear portion of the stress-strain curve, which corresponds to the stress divided by the strain of the film sample. Ten specimens from each film were used and the average values were presented.

2.8. Water vapor permeability

The water vapor permeability (WVP) of films was determined gravimetrically following the standard method of ASTM E96-95 with modification (Gennadios, Weller, & Gooding, 1994). The cup made of poly(methylmethacrylate) with an average depth of 2.5 cm and inside diameter of 6.8 cm was used to measure WVP. Films were cut into rectangular shape (7.5 cm × 7.5 cm) and directly placed on the top of cups containing 18 mL of water. The rim was placed on each cup with film and tightened using screws to prevent leakage of water vapor. The entire cup was weighed and subsequently placed in a humidity chamber (model FX 1077, Jeio Tech Co., Ltd., Ansan, Korea) set at 25 °C and 50% RH. At every 1 h time interval, the weight loss from each cup was measured for 8 h. The slopes of the steady-state (linear) portion of weight loss versus time curves were used to calculate the water vapor transmission rate (WVTR; g/m^2 s) of the film. Then, the WVP (g.m/m^2 Pa.s) of the film was calculated as follows:

$$\mathrm{WVP} = (\mathrm{WVTR} \times L)/\Delta p \quad (4)$$

where, L was mean thickness of the film (m) and Δp was partial water vapor pressure difference (Pa) across the film which was calculated with the method of Gennadios et al. (1994).

2.9. Water contact angle

Surface hydrophobicity of the film was determined by measuring the water contact angle (CA) of the film surface using a CA analyzer (model Phoenix 150, Surface Electro Optics Co., Ltd., Kunpo, Korea). Films were cut into rectangular pieces (3 cm × 10 cm) and directly placed on the horizontal movable stage (black Teflon coated steel, 7 cm × 11 cm) that fitted with the CA analyzer. A drop of water (ca. 10 μL) was placed on the surface of the film using a microsyringe. The contact angle on both sides of the water droplet was measured to assume symmetry and horizontal level. Three measurements were taken for each sample and average values were presented as the degree of CA.

2.10. Moisture content

Moisture content (MC) of carrageenan and carrageenan/CNF nanocomposite films was determined using a drying oven method (Rhim & Wang, 2013). The rectangular films were cut into square of 3 cm × 3 cm and subsequently dried at 105 °C for 24 h using a drying oven. The MC was calculated from the weight loss and expressed as percent MC.

2.11. Antibacterial activity

Antibacterial activities of neat carrageenan and carrageenan/CNF nanocomposite films were examined as their inhibitory effects against the growth of Gram-positive bacteria, *L. monocytogenes* and Gram-negative bacteria, *Escherichia coli*. In order to study the antibacterial activities, changes of the growth of *L. monocytogenes* and *E. coli* incubated in the broth medium have been investigated following the method of Li, Xing, Jiang, Ding, and Li (2009) and Shankar, Teng, and Rhim (2014). All the strains were aseptically inoculated in TSB and BHI broth and subsequently incubated at 37 °C for 16 h. An inoculums (100 μL) of *L. monocytogenes* and *E. coli* were aseptically transferred to 50 mL of TSB and BHI broth containing film samples (5 × 5 cm^2) and subsequently incubated at 37 °C for 12–16 h under mild shaking. The inhibitory effect was estimated periodically by measuring turbidity of the cultured medium at 600 nm using a spectrophotometer. The experiment was performed in triplicate with individually prepared films.

2.12. Statistical analysis

The measurements of each property of the films were performed in triplicate with individually prepared film samples as the replicated experimental units, and mean values with standard deviations (SD) were reported. One-way analysis of variance (ANOVA) was performed, and the significance of each mean property value was determined ($p < 0.05$) with the Duncan's multiple range test using the SPSS statistical analysis computer program for Windows (ver. 12.0, SPSS Inc., Chicago, IL, USA).

3. Results and discussion

3.1. Isolation of chitin nanofibrils

The chitin was pale reddish flake like structure which upon acid hydrolysis resulted into a homogeneous milky suspension of CNF. The size of the particles of CNF was in the range of 25–300 nm with poly dispersity index of 0.356 ± 0.048 (data not shown). A high distribution of particle size of CNF might be due to the presence of fibrous forms of CNF. The size and distribution of the particles depend not only on the structure of the source, but also on the acid concentration, temperature, time of acid hydrolysis, and the mechanical treatment (Das et al., 2009). The results indicate that the chitin has been hydrolyzed into nanofibrils.

3.2. Morphology

Microstructure of chitin, CNF, carrageenan film, and carrageenan/CNF nanocomposite films was observed by the SEM (data not shown). The surface morphology of chitin showed many fibrillar structures bound to each other. The crab shells consist of highly mineralized chitin-protein fibers arranged in a twisted plywood pattern (Chen, Lin, McKittrick, & Meyers, 2008). Chitin has been known to form microfibrillar arrangements embedded in a protein matrix, and these microfibers have diameters ranging from 2.5 to 2.8 nm (Gardner & Blackwell, 1975). The chitin was converted into needle or rod shaped CNF after acid hydrolysis, homozinization, and sonication. The SEM image also showed that the fibers of CNF were separated from each other and well dispersed. The estimated average length of CNF was 150–200 nm and diameter of CNF was around 5–10 nm.

Carrageenan and carrageenan/CNF nanocomposite films prepared by the solvent casting method were free-standing, flexible, and homogeneous. The neat carrageenan film displayed smooth surface which indicated the formation of homogeneous film. On the other hand, the carrageenan/CNF nanocomposite films showed discrete CNF particles in the carrageenan matrix (data not shown). CNF were dispersed uniformly in the polymer matrix when 3% and 5% of CNF were used for reinforcement. However, at higher concentration of CNF (10 wt%) in carrageenan matrix resulted in non-uniform distribution and agglomeration of CNF, which led to the rough surface of films. The results indicated that reinforcement 5 wt% of CNF is the optimum concentration to prepare carrageenan/CNF nanocomposite films.

3.3. Fourier transform infrared analysis

The FT-IR spectra of the chitin and CNF are shown in Fig. 1. All the spectra matched well with the previously reported spectrum of chitin (Muzzarelli et al., 2007). The FT-IR spectrum of chitin showed the O—H and N—H stretching band at 3440 and 3257 cm^{-1}, respectively. The peaks at 1654 and 1625 cm^{-1} attributed to the amide band I, which indicated the presence of α-chitin structure (Ravindra, Krovvidi, & Khan, 1998). The amide II band position was observed at 1562 cm^{-1}. An intense peak observed at 1378 and 1314 cm^{-1} corresponds to a C—H stretch of methyl groups, however, peak observed at 1260 cm^{-1} was attributed to Amide III of the acetyl group. The doublet peaks at 1152–1156 cm^{-1} were ascribed to glycosidic linkage and C—H stretching vibration. The intense peaks at 1018–1070 cm^{-1} were due to the saccharide structure of carbohydrate backbone. The peak at 898 cm^{-1} confirmed the presence of a glycopyranose link of chitin (Yen, Yang, & Mau, 2009). The intensity of the peaks of the CNF decreased slightly compared to those of the chitin, however, no change in peak positions were observed. The results suggested that the basic chemical structure of chitin was maintained even after acid hydrolysis, homogenization, and ultrasonic treatments.

3.4. X-ray diffraction analysis

The crystal structure of chitin and CNF was tested using the XRD as shown in Fig. 2a. The chitin exhibited its characteristic crystalline peaks around $2\theta = 9.1^\circ$ and 19.1° (Cardenas, Cabrera, Taboada, & Miranda, 2004). The diffraction peak of CNF appeared at $2\theta = 19.2^\circ$ was more intense than that of chitin, indicating an increase in the crystallinity of CNF. On the contrary, other two peaks at 10.2° and 28° almost disappeared. The degree of crystallinity (DC), determined using Eq. (1), increased from 81.1% (chitin) to 88.6% (CNF). The increase in the crystallinity of the CNF was presumably due to the removal of amorphous portions from the chitin and realignment of nanocrystals during acid hydrolysis (Li et al., 2009; Reddy & Rhim, 2014b). The crystallite size of the chitin and CNF calculated using the Scherrer equation was 4.73 and 6.27 nm, respectively. The crystallite size of chitin had increased slightly after acid hydrolysis. It has been reported that the crystallite size of cellulose nanocrystals prepared by acid hydrolysis of cellulose was higher that that of untreated cellulose fiber (Maiti et al., 2013; Reddy & Rhim, 2014b).

The XRD patterns of the carrageenan and carrageenan/CNF nanocomposite films are shown in Fig. 2b. The XRD patterns of carrageenan films exhibited a broad diffraction peak from 10° to 24°. However, the XRD patterns of the carrageenan/CNF composite films were different from those of the neat carrageenan film. The intensity of peak at 2θ of 19.1° increased significantly with an increase in the concentration of CNF. These results suggest that the increase in crystallinity of carrageenan/CNF nocomposite films was due to the higher concentration of crystalline CNF in the polymer matrix.

3.5. Thermal stability analysis

The TGA analysis result on chitin and CNF were shown in Fig. 3a. The TGA of chitin and CNF revealed two main weight loss regions. The first region at a temperature of 80–120 °C was due to the evaporation of physically weak and chemically strong bound water, and the weight loss of the film in this range was about 10 wt%. The second transition region was observed at around 300–400 °C, which could be attributed to the degradation of the saccharide structure of the molecule, dehydration of saccharide rings, and the polymerization and decomposition of the acetylated and deacetylated units of chitin (Peesan, Rujiravanit, & Supaphol, 2003). The total weight loss in those ranges was about 70% and 85% for the CNF and chitin, respectively. The TGA results in the main thermal degradation region clearly exhibited that the CNF was less thermostable than the chitin. The same trend of decreased thermal stability was also observed with cellulose nanocrystals isolated from garlic skin fiber by the acid hydrolysis using sulfuric acid (Reddy & Rhim, 2014a). This is probably due to the introduction of sulfate groups into the crystalline chitin during sulfuric acid hydrolysis. The sulfate groups introduced to the outer surfaces of chitin caused dehydration to reduce thermal stability (Roman & Winter, 2004). DTG curves clearly show the maximum decomposition temperature of chitin and CNF, which were observed at 391 and 381 °C, respectively (Fig. 3b). Final residue of chitin and CNF at 600 °C were 19.2% and 25%, respectively.

3.6. Apparent color and transmittance of films

All the carrageenan and carrageenan/CNF nanocomposite films were flexible and highly transparent with smooth surface. The apparent color and transparency of the films determined by the Hunter *Lab*-values and the percent transmittance at visible light (660 nm), respectively, were presented in Table 1. The color values and transmittance of carrageenan/CNF nanocomposite films were significantly ($p < 0.05$) different from those of carrageenan film and they were also affected by the concentration of CNF included. Lightness (*L*-value) and transmittance of the composite films decreased linearly, while greenness (*a*-value), yellowness (*b*-value), and total color difference (ΔE) of the composite films increased monotonously with increase in the content of the CNF.

3.7. Tensile properties of films

The mechanical properties of the carrageenan and carrageenan/CNF naocomposite films determined by the tensile test were shown in Table 2. Thickness of the film increased linearly with increase in the content of CNF, which was mainly due to the increase in the solid content of the film. The TS value of the

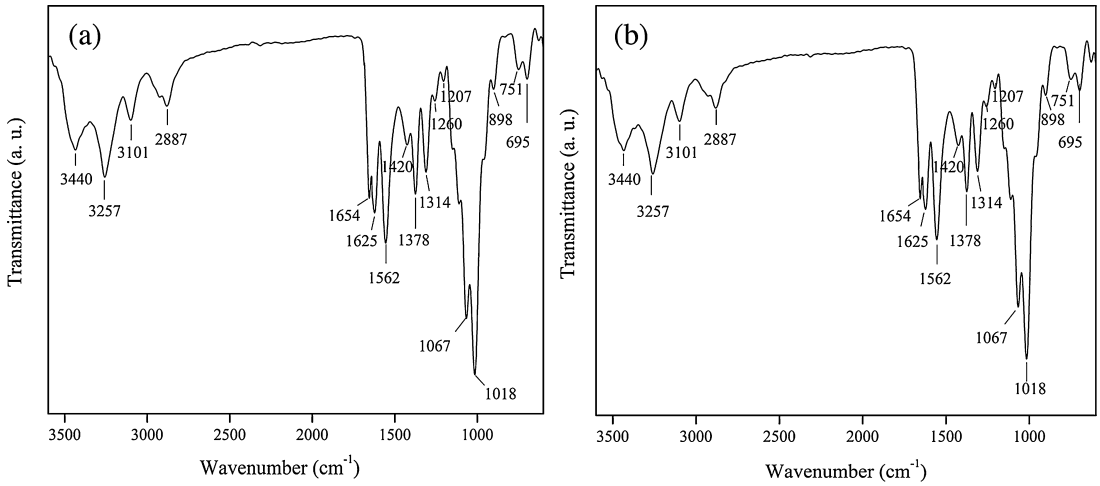

Fig. 1. FTIR spectra of (a) chitin and (b) chitin nanofibrils.

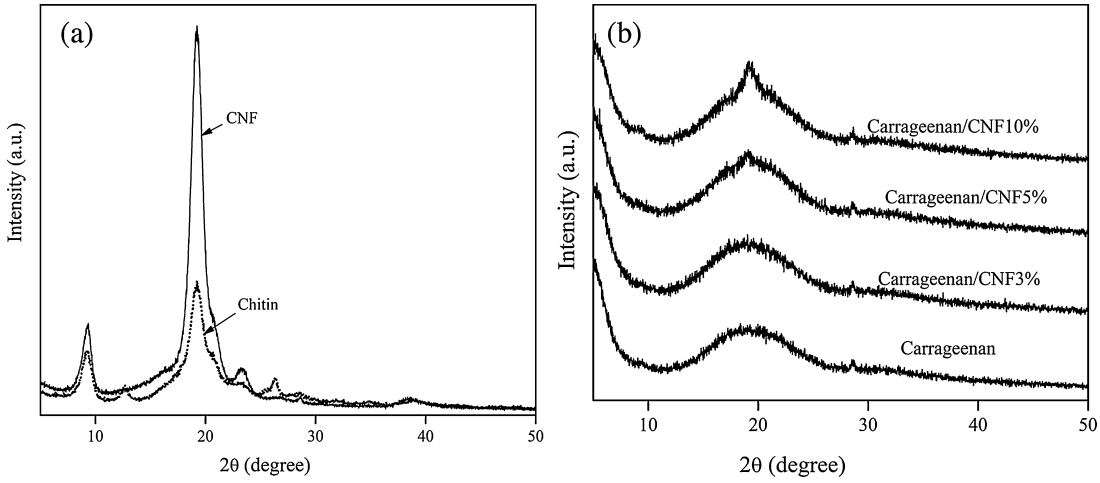

Fig. 2. XRD patterns of (a) chitin and chitin nanofibrils and (b) carrageenan/CNF nanocomposite films.

composite films increased from 30.2 ± 1.8 to 44.7 ± 3.6 MPa with increase in the CNF concentration from 0 to 5 wt%, then decreased with more addition of CNF. However, the stiffness of the film determined by the elastic modulus (EM) increased linearly with increase in the CNF content. The increase in TS and YM of the composite films by blending with the CNF might be attributed to the reinforcement effect of homogeneously dispersed high-strength CNF in the carrageenan polymer matrix. The reinforcing effect of the CNF is mainly due to their high stiffness and strength (Mincea et al., 2012), and the increase in the mechanical properties of polymer/CNF nanocomposite films, presumably resulted from the formation of a percolating network based on hydrogen bonding

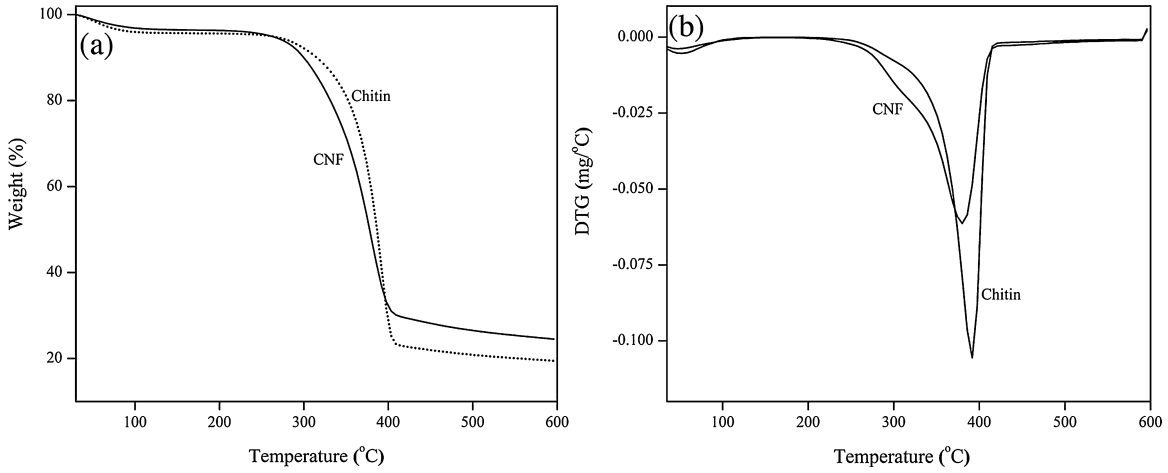

Fig. 3. TGA thermograms (a) and DTG curves (b) of chitin and chitin nanofibrils.

Table 1
Apparent color and transmittance of carrageenan and carrageenan/CNF nanocomposite films*.

Film	L	a	b	ΔE	$T_{660\,nm}$ (%)
Carrageenan	93.4 ± 0.2[a]	−0.34 ± 0.01[a]	4.10 ± 0.01[d]	3.52 ± 0.10[d]	90.4 ± 0.2[a]
Carrageenan/CNF3%	93.2 ± 0.1[b]	−0.34 ± 0.01[a]	4.21 ± 0.02[c]	3.95 ± 0.07[c]	88.4 ± 0.1[b]
Carrageenan/CNF5%	92.5 ± 0.3[b]	−0.50 ± 0.02[b]	4.50 ± 0.13[b]	4.63 ± 0.0b[c]	86.1 ± 0.5[c]
Carrageenan/CNF10%	91.8 ± 0.4[c]	−0.58 ± 0.03[c]	4.70 ± 0.03[a]	5.09 ± 0.18[a]	77.7 ± 0.2[d]

* Each value is the mean of three replicates with standard deviation. Any two means in the same column followed by the same superscript letter are not significantly ($p > 0.05$) different by Duncan's multiple range test.

Table 2
Tensile properties of carrageenan/CNF nanocomposite films*.

Film	Thickness (μm)	TS (MPa)	EM (GPa)	E (%)
Carrageenan	53.5 ± 2.1[d]	30.2 ± 1.8[c]	1.07 ± 0.09[d]	21.8 ± 1.8[a]
Carrageenan/CNF3%	59.2 ± 1.9[c]	40.7 ± 3.5[b]	1.43 ± 0.08[c]	14.4 ± 2.6[b]
Carrageenan/CNF5%	62.2 ± 1.6[b]	44.7 ± 3.6[a]	1.56 ± 0.09[b]	11.2 ± 1.3[c]
Carrageenan/CNF10%	66.8 ± 2.0[a]	29.8 ± 3.5[c]	1.77 ± 0.09[a]	3.9 ± 1.6[d]

* Each value is the mean of three replicates with the standard deviation. Any two means in the same column followed by the same superscript letter are not significantly ($p > 0.05$) different by Duncan's multiple range test.

Table 3
Moisture content, water vapor permeability and water contact angle of carrageenan/CNF nanocomposite films*.

Film	MC (%, w.b.)	WVP ($\times 10^{-9}$ g.m/m^2 Pa.s)	CA (deg.)
Carrageenan	15.3 ± 0.1[a]	1.91 ± 0.03[a]	61.3 ± 0.5[a]
Carrageenan/CNF3%	14.2 ± 0.8[bc]	1.63 ± 0.01[c]	58.8 ± 0.3[b]
Carrageenan/CNF5%	13.9 ± 0.3[c]	1.54 ± 0.01[d]	55.7 ± 1.3[c]
Carrageenan/CNF10%	14.4 ± 1.2[b]	1.71 ± 0.02[b]	53.5 ± 0.7[d]

* Each value is the mean of three replicates with the standard deviation. Any two means in the same column followed by the same superscript letter are not significantly ($p > 0.05$) different by Duncan's multiple range test.

forces (Dufresne, 2010). However, TS of the composite film declined when CNF concentration increased to 10 wt%. Chang, Jian, Yu, and Ma (2010) also found similar result with starch/chitosan nanparticles composite films that the TS of the composite films increased with increase in the filler content up to 6%, then it decreased with more than 6% of nanofillers. The decrease in TS with high content of CNF may probably due to the agglomeration of CNF or non-homogeneous dispersion of CNF at high concentration caused by the self-networking of the nanowhiskers (Agustin et al., 2013). This phenomenon can be greatly influenced by the aspect ratio of the nanoparticle, processing methods, and the resulting interaction between polymer matrix and filler.

On the contrary, the flexibility of the composite films determined by the elongation at break (E) decreased linearly with increase in the CNF content. This may be caused by the rigid nature of the nanofillers (Mincea et al., 2012; Reddy & Rhim, 2014b). The incorporation of CNF restricts the motion of the carrageenan matrix in the terms of the strong interactions between the fillers and the bio-polymer matrix.

3.8. Water vapor permeability and water contact angle of films

Moisture content (MC), water vapor permeability (WVP), and water contact angle (CA) of carrageenan and carrageenan/CNF nanocomposite films were presented in Table 3. The MC of carrageenan films decreased significantly ($p < 0.05$) after blending with CNF, and the MC decreased linearly up to 5 wt% of CNF, then increased with higher content of CNF (10 wt%). The decrease in MC of the composite films may be due to the inclusion of the crystalline form of CNF with less hydrated. The WVP of the films exhibited a similar pattern of decrease with inclusion of CNF. The WVP of neat carrageenan was 1.91×10^{-9} g.m/m^2 Pa.s, and it decreased significantly ($p < 0.05$) after formation of nanocomposite with CNF. It showed the minimum value of 1.54×10^{-9} g.m/m^2 Pa s when 5 wt% of CNF included, then increased again with higher content of CNF (10 wt%). Similar dependence on the nanofiller content on the WVP has been observed with cellulose nanocrystal included agar films (Reddy & Rhim, 2014b) and chitosan nanoparticles reinforced starch films (Chang et al., 2010). The decrease in WVP of the composite films at low filler content may be attributed to the tortuous path of water vapor diffusion through the polymer matrix and thus decreased in WVP, which was caused by the impermeable crystalline chitin molecules dispersed well in the carrageenan polymer matrix (Reddy & Rhim, 2014b). However, when more than 5 wt% of CNF were included, they were aggregated to result in decreased effective filler content and facilitated water vapor permeation (Chang et al., 2010).

The CA is usually used as a measure of a basic wetting property of polymer which measures the degree of hydrophilicity or hydrophobicity of the film surface. The CA of carrageenan and carrageenan/CNF nanocomposite films are also shown in Table 3. Usually, films with less than 65° of CA is considered as hydrophilic (Vogler, 1998). The CA of the neat carrageenan film was 61.3°, therefore it can be considered as hydrophilic. The hydrophilic property of the carrageenan film may be mainly attributed to its functional hydrophilic hydroxyl and carboxyl groups. The CA of carrageenan/CNF nanocomposite films decreased significantly ($p < 0.05$) compared with the near carrageenan film, which decreased down to 53.5° with 10 wt% of CNF. Moreover, the decrease in CA of the composite films depended on the content of CNF. The similar result was observed, when cellulose nanocrystals were incorporated into the agar film (Reddy & Rhim, 2014b). This decrease in the CA value of carrageenan film with CNF addition could be attributed to the highly polar and hydrophilic nature of CNF.

3.9. Antibacterial activity

Antimicrobial activity of carrageenan and carrageenan/CNF nanocomposite films against *L. monocytogenes* and *E. coli* was evaluated by measuring the optical density (OD, absorbance at 600 nm) of culture medium including the test films and microorganisms, and the results are shown in Fig. 4. Since the OD of the medium increase with growth of microorganisms, lower absorbance at 600 nm indicates higher antibacterial activity of the test material. As expected, the neat carrageenan film did not show any antimicrobial activity against both organisms, *L. monocytogenes* and *E. coli* bacteria. However, the CNF included carrageenan films exhibited distinctive

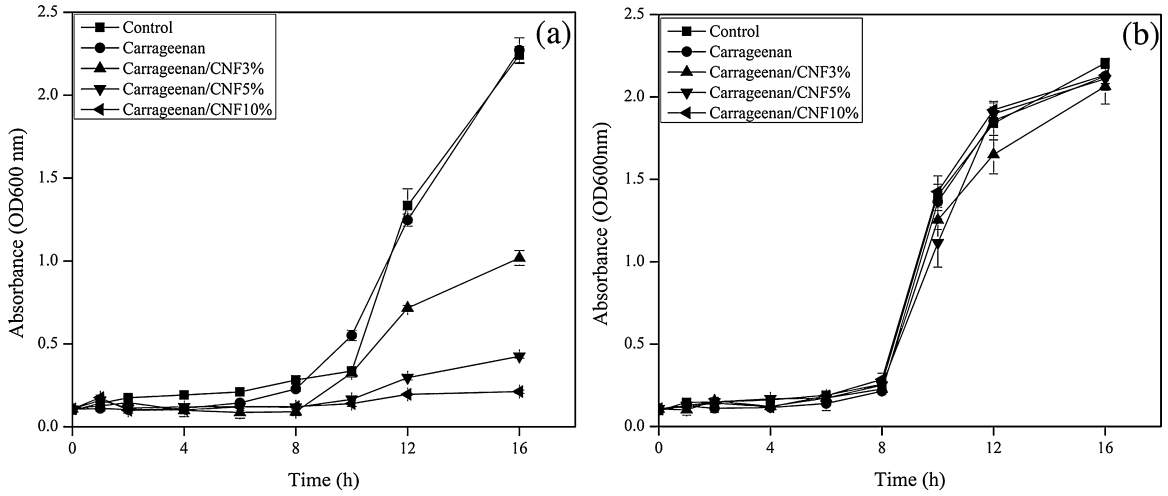

Fig. 4. Antimicrobial activity of carrageenan and carrageenan/CNF nanocomposite films against (a) *L. monocytogenes* and (b) *E. coli*.

antimicrobial activity against *L. monocytogenes*, but their antimicrobial activity against *E. coli* was not so distinctive. Moreover, the antimicrobial activity of carrageenan/CNF nanocomposite films against *L. monocytogenes* depended on the content of CNF. The results coincided with the previous report that CNF could be characterized as bacteriostatic rather than bactericidal. Though the clear mechanism of the antibacterial activity of CNF has not been explained yet, the CNF probably makes the bacteria flocculate and prevent growth presumably through lack of nutrients and oxygen (i.e. mass transfer limitation). However, at the tested concentrations (3, 5, and 10 wt%) of CNF, there may have been insufficient free polysaccharide to flocculate and kill all of the bacteria in the culture medium, thus the surviving cells would have gone on reproduction (Benhabiles et al., 2012). The other possible antimicrobial mechanism involves the interactions between positively charged chitin and negatively charged bacterial cell membranes, which results in increased membrane permeability and eventually causing rupture and leakage of intracellular material (de Azeredo, 2009).

4. Conclusions

Fibrous type of CNF was isolated from chitin obtained from crab shell by the acid hydrolysis, high spend homogenization, and ultrasonication. The CNF was used as a reinforcement filler for the preparation of carrageenan/CNF nanocomposite films. The carrageenan/CNF nanocomposite films showed improved physical, mechanical, and water vapor barrier properties compared to the neat carrageenan film up to the inclusion of 5 wt% of CNF. In addition, the CNF included carrageenan films exhibited strong antimicrobial activity against *L. monocytogenes*. These results suggest that the CNF with antimicrobial activity can be used as a reinforcing nanofiller to improve film properties of biopolymer-based packaging films to secure food safety and to prolong the shelf-life of packaged foods.

Acknowledgments

This research was supported by the Agriculture Research Center (ARC 710003) program of the Ministry for Agriculture, Food and Rural Affairs, Korea.

References

Agustin, M. B., Ahmmad, B., Richel, E. P. D. L., Jerico, L. B., Joel, R. S., & Fumihiko, H. (2013). Starch-based biocomposite films reinforced with cellulose nanocrystals from garlic stalks. *Polymer Composites*, *34*, 1325–51332.

Benhabiles, M. S., Salah, R., Lounici, H., Drouichea, N., Goosend, M. F. A., & Mameri, N. (2012). Antibacterial activity of chitin, chitosan and its oligomers prepared from shrimp shell waste. *Food Hydrocolloids*, *29*, 48–56.

Cardenas, G., Cabrera, G., Taboada, E., & Miranda, S. P. (2004). Chitin characterization by SEM, FTIR, XRD, and ^{13}C cross polarization/mass angle spinning NMR. *Journal of Applied Polymer Science*, *93*, 1876–1885.

Chang, P. R., Jian, R., Yu, J., & Ma, X. (2010). Fabrication and characterization of nanoparticles/plasticized-starch composites. *Food Chemistry*, *120*, 736–740.

Chen, P. Y., Lin, A. Y. M., McKittrick, J., & Meyers, M. A. (2008). Structure and mechanical properties of crab exoskeletons. *Acta Biomaterialia*, *4*, 587–596.

Das, K., Ray, D., Bandyopadhyay, N. R., Ghosh, T., Mohanty, A. K., & Misra, M. (2009). A study of the mechanical, thermal and morphological properties of microcrystalline cellulose particles prepared from cotton slivers using different acid concentrations. *Cellulose*, *16*, 783–793.

de Azeredo, H. M. C. (2009). Nanocomposites for food packaging applications. *Food Research International*, *42*, 1240–1253.

Dufresne, A. (2010). Processing of polymer nanocomposites reinforced with polysaccharide nanocrystals. *Molecules*, *15*, 4111–4128.

El-Nesr, E. M., Raafat, A. I., Nasef, S. M., Soliman, E. A., & Hegazy, E. A. (2013). Chitin and chitosan extracted from irradiated and non-irradiated shrimp wastes (comparative analysis study). *Arab Journal of Nuclear Science and Applications*, *46*, 53–66.

Gardner, K. H., & Blackwell, J. (1975). Refinement of the structure of â chitin. *Biopolymers*, *14*, 1581–1595.

Gennadios, A., Weller, C. L., & Gooding, C. H. (1994). Measurement errors in water vapor permeability of highly permeable, hydrophilic edible films. *Journal of Food Engineering*, *21*, 395–409.

Ifuku, S., Nogi, M., Abe, K., Yoshioka, M., Morimoto, M., Saimoto, H., et al. (2009). Preparation of chitin nanofibers with a uniform width as α-chitin from crab shells. *Biomacromolecules*, *10*, 1584–1588.

Li, X., Xing, Y., Jiang, Y., Ding, Y., & Li, W. (2009). Antimicrobial activities of ZnO powder-coated PVC film to inactivate food pathogens. *International Journal of Food Science and Technology*, *44*, 2161–2168.

Maiti, S., Jayaramudu, J., Das, K., Reddy, S. M., Sadiku, R., Ray, S. S., et al. (2013). Preparation and characterization of nano-cellulose with new shape from different precursor. *Carbohydrate Polymers*, *98*, 562–567.

Martins, J. T., Bourbon, A. I., Pinheiro, A. C., Souza, B. W. S., Cerqueira, M. A., & Vicente, A. A. (2013). Biocomposite films based on κ-carrageenan/locust bean gum blends and clays: physical and antimicrobial properties. *Food and Bioprocess Technology*, *6*, 2081–2092.

Mincea, M., Negrulescu, A., & Ostafe, V. (2012). Preparation, modification, and applications of chitin nanowhiskers: A review. *Reviews on Advanced Materials Science*, *30*, 225–242.

Muzzarelli, R. A. A. (2011a). Chitin nanostructures in living organisms. In N. S. Gupta (Ed.), *Chitin formation and diagenesis. Topics in geobiology* (pp. 1–34). New York: Springer.

Muzzarelli, R. A. A. (2011b). Biomedical exploitation of chitin and chitosan via mechano-chemical disassembly, electrospinning, dissolution in imidazolium ionic liquids, and supercritical drying. *Marine Drugs*, *9*, 1510–1533.

Muzzarelli, R. A. A. (2012). Nanochitins and nanochitosans, paving the way to eco-friendly and energy-saving exploitation of marine resources. *Polymer Science: A Comprehensive Reference*, *10*, 153–164.

Muzzarelli, R. A. A., Boudrant, J., Meyer, D., Manno, N., DeMarchis, M., & Paoletti, M. G. (2012). Current views on fungal chitin/chitosan, human chitinases, food preservation, glucans, pectins and inulin: A tribute to Henri Braconnot, precursor of the carbohydrate polymers science, on the chitin bicentennial. *Carbohydrate Polymers*, *87*, 995–1012.

Muzzarelli, R. A. A., Morganti, P., Morganti, G., Palombo, P., Palombo, M., Biagini, G., et al. (2007). Chitin nanofibrils/chitosan glycolate composites as wound medicaments. *Carbohydrate Polymers*, *70*, 274–284.

Necas, J., & Bartosikova, L. (2013). Carrageenan: A review. *Veterinarni Medicina*, *58*, 187–205.
Peesan, M., Rujiravanit, R., & Supaphol, P. (2003). Characterization of beta-chitin/poly(vinyl alcohol) blend films. *Polymer Testing*, *22*, 381–387.
Ravindra, R., Krovvidi, K. R., & Khan, A. A. (1998). Solubility parameter of chitin and chitosan. *Carbohydrate Polymers*, *36*, 121–127.
Reddy, J. P., & Rhim, J. W. (2014a). Isolation and characterization of cellulose nanocrystals from garlic skin. *Materials Letters*, *129*, 20–23.
Reddy, J. P., & Rhim, J. W. (2014b). Characterization of bionanocomposite films prepared with agar and paper-mulberry pulp nanocellulose. *Carbohydrate Polymers*, *110*, 480–488.
Revol, J. F., & Marchessault, R. H. (1993). In vitro chiral nematic ordering of chitin crystallites. *International Journal of Biological Macromolecules*, *15*, 329–335.
Rhim, J. W., Park, H. M., & Ha, C. S. (2013). Bio-nanocomposites for food packaging applications. *Progress in Polymer Science*, *38*, 1629–1652.
Rhim, J. W. (2011). Effect of clay contents on mechanical and water vapor barrier properties of agar-based nanocomposite films. *Carbohydrate Polymers*, *86*, 691–699.
Rhim, J. W. (2012). Physical-mechanical properties of agar/κ-carrageenan blend film and derived clay nanocomposite film. *Journal of Food Science*, *77*, 66–73.
Rhim, J. W., & Wang, L. F. (2013). Mechanical and water barrier properties of agar/κ-carrageenan/konjac glucomannan ternary blend biohydrogel films. *Carbohydrate Polymers*, *96*, 71–81.
Roman, M., & Winter, W. T. (2004). Effect of sulfate groups from sulfuric acid hydrolysis on the thermal degradation behavior of bacterial cellulose. *Macromolecules*, *5*, 1671–1677.
Shankar, S., Teng, X., & Rhim, J. W. (2014). Properties and characterization of agar/CuNP bionanocomposite films prepared with different copper salts and reducing agents. *Carbohydrate Polymers*, *114*, 484–492.
Vogler, E. A. (1998). Structure and reactivity of water at biomaterial surfaces. *Advances in Colloid and Interface Science*, *74*, 69–117.
Yen, M. T., Yang, J. H., & Mau, J. L. (2009). Physicochemical characterization of chitin and chitosan from crab shells. *Carbohydrate Polymers*, *75*, 15–21.